CO2 and temperature decoupling at the million-year scale during the Cretaceous Greenhouse

Abel Barral, Bernard Gomez, François Fourel, Véronique Daviero-Gomez, Christophe Lecuyer

SCIENTIFIC REPORTS

OPEN

CO_2 and temperature decoupling at the million-year scale during the Cretaceous Greenhouse

Received: 17 March 2017
Accepted: 10 July 2017
Published online: 23 August 2017

Abel Barral[1], Bernard Gomez[1], François Fourel[1], Véronique Daviero-Gomez[1] & Christophe Lécuyer[1,2]

CO_2 is considered the main greenhouse gas involved in the current global warming and the primary driver of temperature throughout Earth's history. However, the soundness of this relationship across time scales and during different climate states of the Earth remains uncertain. Here we explore how CO_2 and temperature are related in the framework of a Greenhouse climate state of the Earth. We reconstruct the long-term evolution of atmospheric CO_2 concentration (pCO_2) throughout the Cretaceous from the carbon isotope compositions of the fossil conifer *Frenelopsis*. We show that pCO_2 was in the range of ca. 150–650 ppm during the Barremian–Santonian interval, far less than what is usually considered for the mid Cretaceous. Comparison with available temperature records suggest that although CO_2 may have been a main driver of temperature and primary production at kyr or smaller scales, it was a long-term consequence of the climate-biological system, being decoupled or even showing inverse trends with temperature, at Myr scales. Our analysis indicates that the relationship between CO_2 and temperature is time scale-dependent at least during Greenhouse climate states of the Earth and that primary productivity is a key factor to consider in both past and future analyses of the climate system.

Greenhouse gas emissions resulting from human activity are considered to be an important driver of the current global warming. Accurate understanding of this cause-effect relationship is essential to propose realistic scenarios of the future evolution of Earth's climate, but the human monitoring history of these variables may be very tenuous to properly take into account the relative importance of their large time-scale dynamics into the climate system. Geological records offer an opportunity to address this time-scale issue as they provide track of the long-term dynamics of atmospheric greenhouse gas contents and surface temperature throughout Earth's history. An analysis of this relationship throughout the whole Phanerozoic pointed out atmospheric pCO_2 as the main multi-scale driver of global warming[1]. However, recent improvement and refining of methods to reconstruct pCO_2 evidence that this conclusion was based on outdated imprecise estimates[2,3]. Additionally, some factors involved in long-term climate dynamics such as O_2 have been put forward to challenge this paradigm[4]. This raises questions about the extent to which we are correctly interpreting the relative influence of atmospheric pCO_2 forcing on climate[5].

The analysis of the relationship between pCO_2 and temperature for the Phanerozoic as a whole may not be pertinent because it comprised shifts between drastically different climate states of the Earth in which the relative impact and the dynamics of atmospheric CO_2 may have strongly differed. Of these, Greenhouse is considered to be the default planetary climate state of the Earth, prevailing in more than 70% of the Phanerozoic[6]. The Cretaceous is one of the longest and most studied Greenhouse periods of Earth's history, with an extensive background of pCO_2[7–10] and temperature[11–13] reconstructions. This makes the Cretaceous an exceptional 'laboratory' of the past to explore the relationship between the two factors. Nevertheless, pCO_2 reconstructions made so far for the Cretaceous defined temporal trends that are not consistent with those described for temperature[11–13] or the carbon cycle dynamics evidenced by carbon isotopes[14–16]. This raises questions about how accurate are pCO_2 reconstructions made so far and how significant was the relative contribution of pCO_2 to temperature evolution during the Cretaceous.

[1]Laboratoire de Géologie de Lyon, CNRS UMR 5276, Université Lyon 1, Villeurbanne, 69622, France. [2]Institut Universitaire de France, Paris, France. Correspondence and requests for materials should be addressed to A.B. (email: abel.barral.cuesta@gmail.com)

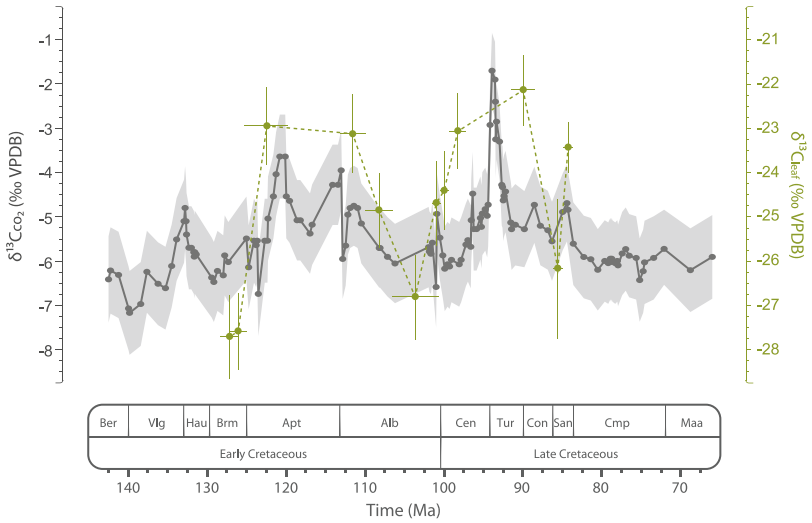

Figure 1. Comparison of the carbon isotope compositions of leaves of the fossil conifer *Frenelopsis* ($\delta^{13}C_{leaf}$) obtained for each studied episode with the evolution of the carbon isotope composition of atmospheric CO_2 ($\delta^{13}C_{CO2}$) throughout the Cretaceous estimated by Barral *et al.*[16]. Envelopes and bar errors correspond to $\pm 1\sigma$.

Carbon isotopes are relevant tools for describing past carbon cycle and CO_2 dynamics[14–20]. Carbon isotope compositions of terrestrial plants are particularly interesting as they are strongly linked to atmospheric CO_2, which is the main source of carbon assimilated by plants via photosynthesis. The recent construction of models relating carbon isotope fractionation by plants and pCO_2[19–21] coupled with the good preservation of the pristine carbon isotope signal within plant fossil materials[22–25], make carbon isotope compositions of plant fossils valuable proxies to analyze the evolution of atmospheric pCO_2 during past periods.

Herein the long-term evolution of atmospheric pCO_2 during the Cretaceous is reconstructed based on the carbon isotope compositions of leaves of the fossil conifer *Frenelopsis* ($\delta^{13}C_{leaf}$). pCO_2 is estimated from twelve stages spanning the Barremian–Santonian interval (129.4–83.6 Ma) during which major disturbance events of the carbon cycle related to CO_2 release to the atmosphere[14,15,18] and major variations in temperature[11–13] described for the Cretaceous took place. We explore the correspondence between estimated pCO_2 trends and those previously published for temperature to analyze the relative influence of pCO_2 forcing on climate during the Cretaceous.

Results and Discussion

Carbon isotope compositions of the fossil conifer *Frenelopsis*. $\delta^{13}C_{leaf}$ values from the twelve studied stages range from −27.7 to −22.1‰ in average (Fig. 1; Table 1). In most of these stages, $\delta^{13}C_{leaf}$ values show similar standard deviations (ca. 0.9‰), thus reflecting a similar range of local environmental variability. Santonian stages are the only exceptions, which may reflect higher climatic instability related to the development of Oceanic Anoxic Event (OAE) 3. Carbon isotope compositions of *Frenelopsis* in the Barremian, upper Albian and lower Santonian stages are notably ^{13}C-depleted compared to others, even though it is not significant in the latter case (Fig. 1). These lower $\delta^{13}C_{leaf}$ values are consistent with decreases in the carbon isotope composition of atmospheric CO_2 ($\delta^{13}C_{CO2}$) recently described by Barral *et al.*[16] (Fig. 1). Overall, there is a good agreement between $\delta^{13}C_{leaf}$ and $\delta^{13}C_{CO2}$ curves, though trends in the former are generally magnified. This magnification is more pronounced during the Cenomanian-Turonian interval, coinciding with a critical increase in global temperatures[11], which may have slightly reduced carbon isotope fractionation by plants ($\Delta^{13}C_{leaf}$) by reducing the discrimination effect of RuBisCO against ^{13}C[26,27].

Atmospheric CO_2 concentration during the Cretaceous. $\Delta^{13}C_{leaf}$ values inferred from $\delta^{13}C_{leaf}$ and concomitant $\delta^{13}C_{CO2}$ values (Table 1) were used to estimate pCO_2 values. pCO_2 estimates are in the range of ca. 150–650 ppm for the Barremian–Santonian interval, and the resolution is better than 55 ppm (i.e. 1σ, standard deviation) for most of the stages (Fig. 2; Table 1). This range of values is consistent with the conclusions by Franks *et al.*[20] from a method based on universal equations of leaf gas exchange using stomatal anatomy and carbon isotope ratios of fossil leaves suggesting pCO_2 values below 1000 ppm during most of the Phanerozoic, although their conclusions remain controversial[28–30]. Our pCO_2 estimates average ca. 300 ppm for the studied interval, which is in accordance with the most recent revision of GEOCARBSULF model[3] and the range of values obtained in most recent works dealing with proxy-based reconstructions[7–10] (Fig. 2). All these reconstructions suggest that atmospheric CO_2 concentrations were comparable to those of present-day atmosphere, which is a conclusion in deep contrast with the classical view that the Cretaceous period was characterized by atmospheric CO_2 concentrations considerably higher than today[31]. This is also consistent with several other approaches. Boron isotope compositions ($\delta^{11}B$) of marine biogenic carbonates are closely related to pCO_2 and pH[32–34]. Higher atmospheric concentrations would imply more CO_2 dissolution into the ocean, causing a lowering of seawater pH and $\delta^{11}B$ of marine biogenic carbonates[33,34]. However, $\delta^{11}B$ of Cretaceous and present-day brachiopods as well as ophiolitic serpentinites are close to each other[35], thus suggesting that seawater pH and atmospheric pCO_2 were of similar

Locality	Age	$\delta^{13}C_{leaf}$ (‰)			$\delta^{13}C_{CO2}$ (‰)		$\Delta^{13}C_{leaf}$ (‰)		pCO_2 (ppm)	
		μ	σ	n	μ	σ	μ	σ	μ	σ
Hautrage	upper lower Barremian–lower upper Barremian	−27.7	0.9	30	−6.1	0.5	22.3	1.1	476.5	135.2
Uña	upper Barremian	−27.6	0.9	30	−5.7	0.7	22.5	1.1	502.2	155.1
Mas de la Parreta	uppermost Barremian–lower Aptian	−23.0	0.9	30	−5.8	0.7	17.6	1.1	191.6	37.6
El Soplao	lower Albian	−23.1	0.9	30	−5.0	0.3	18.6	1.0	225.6	39.4
San Just	lower–middle Albian	−24.9	0.8	30	−5.8	0.5	19.6	1.0	272.3	53.8
Reillo	upper Albian	−26.8	1.0	30	−5.8	0.3	21.6	1.1	408.9	99.0
Archingeay (A1sl–A)	uppermost Albian	−24.7	1.0	26	−5.7	0.4	19.5	1.1	265.8	53.3
Archingeay (A2sm1–2)	lowermost Cenomanian	−24.4	0.9	30	−5.9	0.4	18.9	1.0	240.9	43.9
La Buzinie	uppermost lower–lowermost middle Cenomanian	−23.1	0.9	30	−5.9	0.5	17.6	1.0	190.5	34.5
Infiesto	upper Turonian–Coniacian	−22.1	0.8	30	−5.1	0.4	17.4	0.9	185.0	30.1
Piolenc	lower Santonian	−26.2	1.6	17	−5.2	0.6	21.5	1.7	432.5	220.3
Belcodème	upper Santonian	−23.4	0.6	30	−4.8	0.5	19.1	0.8	246.0	34.5

Table 1. $\delta^{13}C_{leaf}$, $\delta^{13}C_{CO2}$, $\Delta^{13}C_{leaf}$ and pCO_2 values for the twelve studied Cretaceous stages. μ and σ correspond to mean and standard deviation, respectively.

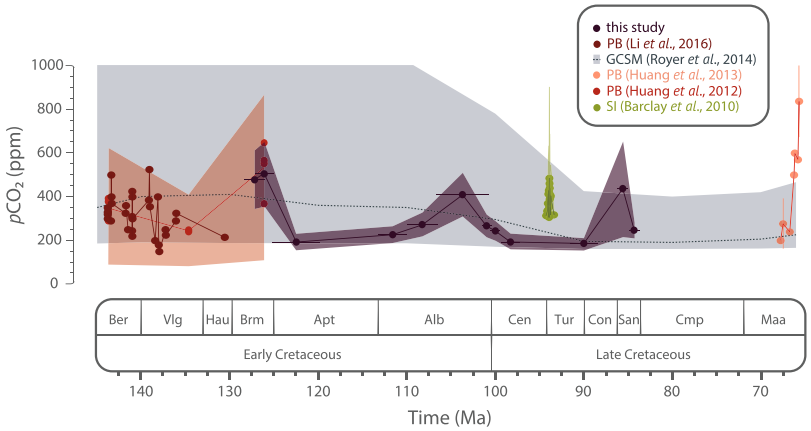

Figure 2. Comparison of the $\delta^{13}C_{leaf}$-based pCO_2 estimates with most recent proxy-based and model-based pCO_2 reconstructions for the Cretaceous[3,7–10]. Envelopes and bar errors represent ±1σ. GCSM: GEOCARBSULF Model reconstructions; PB: Paleosol Barometer reconstructions; SI: Stomatal Index reconstructions.

magnitude. Analysis of reef abundance and diversity throughout the Phanerozoic also agrees with our results, indicating that during the Cretaceous no significant long-term rise in ocean acidification, reflecting a long-term rise in pCO_2, took place[36]. Only discrete short-term events of ocean acidification have been described during the Cretaceous based on marine calcifiers, associated with major Cretaceous OAEs and Hothouse episodes[37,38].

Was pCO_2 a long-term driver of temperature during the Cretaceous? Several events of volcanic CO_2 release into the atmosphere linked to the emplacement of large igneous provinces have been inferred from pronounced negative shifts of both carbon and strontium isotope compositions of marine carbonates[14,38] associated with the main Cretaceous OAEs[14,18,37]. These CO_2 release events are also evident regarding the evolution of $\delta^{13}C_{CO2}$ throughout the Cretaceous[16] (Fig. 1) and are most likely responsible for temperature increases at the kyr scale[12,13]. The biggest of these CO_2 release events in terms of the magnitude of carbon isotope excursions was related to OAE1b and lasted ca. 25 kyr[14,39]. This event was responsible for a fast warming of the atmosphere of ca. 0.3 °C and followed by cooler climatic conditions during a period of ca. 45 kyr[39]. Greater kyr-scale increases in temperature of ca. 6–7 °C have been described associated with the CO_2 release events related to OAE1a[12,13] and OAE2[11] (Fig. 3). However, our results indicate that drastic Myr-scale pCO_2 drawdowns took place during the warmest time intervals described for the Cretaceous[11–13]: a drawdown of ca. 310 ppm (from ca. 500 to ca. 190 ppm) during the upper Barremian-lower Aptian interval (ca. 7.5 Myr), and ca. 225 ppm (from ca. 410 ppm to ca. 190 ppm) during the upper Albian-lower Cenomanian interval (ca. 5 Myr) (Fig. 3). In fact, at the Myr-scale,

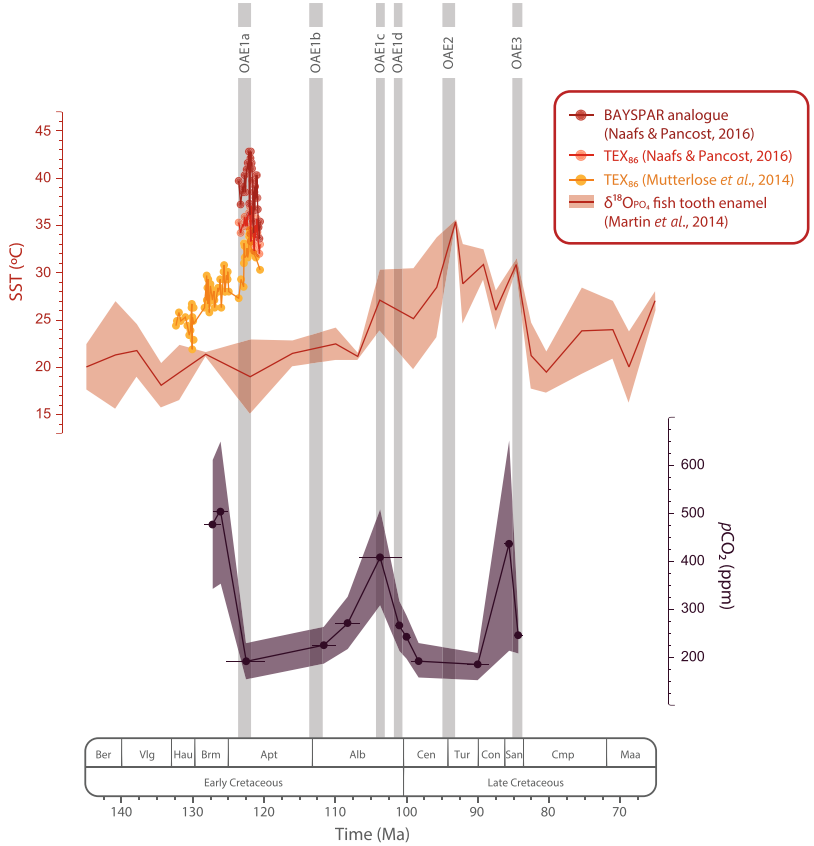

Figure 3. Reconstructed pCO_2 compared with available sea surface temperature (SST) records[11–13] for the Cretaceous. Vertical grey bars represent major Oceanic Anoxic Events (OAE) occurring during the Cretaceous[18]. Envelopes represent $\pm 1\sigma$.

trends in pCO_2 are even inverse compared to temperature during significant time intervals such as the upper Barremian–lower Aptian (considering the higher resolution temperature curves based on TEX_{86} proxy[12,13]) and the upper Albian–Santonian in which pCO_2 minima are coeval with thermal maxima (Fig. 3). If pCO_2 was rather low and usually decoupled from temperature at the Myr-scale, it may not have been the main long-term driver of global warming during the Cretaceous.

Time scale dependency of the relationship between pCO_2 and temperature. Episodes of enhanced primary production have been associated with the kyr-scale CO_2 release events that took place during major OAEs and the warmest intervals of the Cretaceous[40–44]. Barclay *et al.*[7] showed that a 20% increase in pCO_2 during OAE2 triggered extensive primary productivity leading to a global increase in rates of organic carbon burial, which eventually resulted in a pCO_2 decrease down to 26% in ca. 100 kyr. This indicates that, as a consequence of a critical CO_2 release event to the atmosphere, primary productivity can account for pCO_2 drawdowns of at least up to the 10^5 yr scale. The time resolution of our record is not high enough to fully discuss pCO_2 trends on the kyr scale; however, when the time uncertainty of our estimates allows clear perusal, pCO_2 levels are consistently low well after the events of CO_2 release to the atmosphere described in the literature[18,45] (Fig. 3). This indicates that the aforementioned primary productivity effect may exceed the kyr scales resulting in a negative balance or a low-level stasis of pCO_2 up to the Myr scales. If primary production were responsible for a long-term decrease in atmospheric pCO_2 during the Cretaceous, we should find a co-varying increase in atmospheric pO_2 as a product of long-term enhanced photosynthesis. This is in accordance with the long-term trends obtained by the recent revision of the GEOCARBSULF model, which describes both a drawdown of pCO_2 and an increase in pO_2 levels from the earliest stages of the Cretaceous up to the mid Cretaceous[3]. Poulsen *et al.*[4] emphasized the importance of O_2 in long-term climate dynamics as under low pO_2 conditions shortwave scattering by clouds and air molecules is reduced; this implies a significant increase in surface shortwave forcing, leading to increase of atmospheric water vapour and consequent enhanced greenhouse forcing which increases global surface temperatures. Thus, their simulations predict that temperature increases under low pO_2 and high pCO_2 conditions. However, during the Cretaceous temperature was maintained high during the late Albian–Santonian interval coinciding with relatively high pO_2[3] and low pCO_2 conditions[3,7] (Fig. 3). This observation reflects that both pO_2 and pCO_2 parameters may not be enough to explain long-term evolution of temperature.

In addition to the conclusions of previous work on atmospheric CO_2 dynamics at kyr time scales[7] our results indicate that the relationship between CO_2 and temperature was probably scale-dependent during the Cretaceous. In the framework of a Greenhouse climate state functioning, CO_2 appears to have been a main driver of global

warming and primary production at timescales up to the kyr[7]. However, our results indicate that it was decoupled from temperature and most likely a long-term consequence of the climate-biological system at Myr scales. Direct extrapolation of these conclusions to time intervals corresponding to different climate states of the Earth is not pertinent because C cycle dynamics, and thus the evolution of pCO_2, might be strongly modulated by different global scale functioning of climate factors. For instance, temperature strongly affects carbon sequestration by living organisms[26,27], and global oceanic and atmospheric circulation patterns are involved in heat transport[46] and distribution of climate zones[47] that strongly influence primary productivity. Different dynamics and relative effects of those factors within different climate states of the Earth[6] may result in different functioning of atmospheric CO_2 dynamics. However, nowadays anthropogenic CO_2 release into the atmosphere also constitutes a main driver of climate change at a human time scale. At larger scales, primary productivity appears to have been an important driver of atmospheric CO_2 concentration during both interglacial[48] and glacial intervals[49]. Further work on the Myr-scale interrelationships between primary productivity, CO_2 and temperature within these different climate state intervals of the Earth is needed to explore how universal are the conclusions obtained herein. Primary production constitutes a major factor involved in climate dynamics and that regulates the balance between pO_2 and pCO_2. Thus, productivity must be taken into consideration in the evaluation of the relative effect of O_2 and CO_2 on climate dynamics. Present-days anthropogenic CO_2 release event can be compared in magnitude with those of the Cretaceous, reflected in a ca. −1.8‰ shift in $\delta^{13}C_{CO2}$ since the industrial revolution[50] against the ca. −2‰ shift associated with OAE1b[16] (Fig. 1). However, its critically shorter time of development makes it a more intense disturbance event, and so its forthcoming consequences are difficult to predict. Evaluating the response time of primary production to cushion CO_2 forcing will be critical to allow the prediction of climate evolution and its impact in the near future of life on Earth.

Methods

Twelve stages corresponding to eleven sites from the Cretaceous of western Europe were used for pCO_2 reconstruction (see Supplementary Fig. S1). The sites represent similar terrestrial environments in which the fossil conifer genus *Frenelopsis* was present, and they are distributed over a narrow palaeolatitude band (30–40° N) of the same climate zone throughout the time range analyzed[51] (see Supplementary Table S1). These stages and sites were selected to reduce as much as possible environmental biases on $\delta^{13}C_{leaf}$.

Frenelopsis was chosen as a pCO_2 proxy because it was frequent and abundant in Cretaceous ecosystems[52–55]. *Frenelopsis* is a valuable material for performing stable carbon isotope analysis due to its resistance to decay and diagenesis. It provides accurate $\delta^{13}C_{leaf}$ values, which are comparable to those of living plant leaves[25,56,57].

Frenelopsis leaves were treated with HCl 32% following the protocol recommended by Barral *et al.*[25]. Thirty *Frenelopsis* leaves per locality were separately reduced to powder using an agate mortar. Three replicates of ca. 100 μg per leaf were randomly selected and weighted using a precision balance Sartorius ME36S and loaded into tin capsules. Carbon isotope analyses were performed using a continuous flow IRMS configuration, being He the carrier gas, using a EuroEA3028™–HT elemental analyzer working in combustion mode and interfaced with an IP60 isotope ratio mass spectrometer. Carbon isotope ratios were calibrated against the international standard IAEA-C4 ($\delta^{13}C = -23.96$‰) and casein ($\delta^{13}C = -22.67$‰) as an internal reference. Based on repeated analysis of standards, analytical reproducibility was better than ±0.2‰.

pCO_2 values were estimated for each stage using the equation relating pCO_2 to $\delta^{13}C_{leaf}$ described by Schubert and Jahren[19,21] ($r = 0.94$):

$$\Delta^{13}C_{leaf} = [(28.26)(0.22)(pCO_2 + 23.9)]/[28.26 + (0.22)(pCO_2 + 23.9)]$$

$\Delta^{13}C_{leaf}$ values were estimated from $\delta^{13}C_{leaf}$ and concomitant $\delta^{13}C_{CO2}$ values by using the equation proposed by Farquhar *et al.*[58]:

$$\Delta^{13}C_{leaf} = \delta^{13}C_{Co2} - \delta^{13}C_{leaf}/1 + (\delta^{13}C_{co2}/1000)$$

$\delta^{13}C_{CO2}$ values were taken from the $\delta^{13}C_{carb}$-based $\delta^{13}C_{CO2}$ estimates provided by Barral *et al.*[16]. We avoid discrimination bias due to different physiological functioning related to taxonomic specificity by using always the same taxon, and thus $\delta^{13}C_{leaf}$ faithfully represents environmental variability. In order to avoid misrepresented pCO_2 estimates due to subtle uncorrelations between the beds from which $\delta^{13}C_{CO2}$ and $\delta^{13}C_{leaf}$ were obtained, we accounted for $\delta^{13}C_{CO2}$ variability in the uncertainty timespan of the *Frenelopsis* localities by averaging and estimating cumulated error for each stage. This was made by randomly drawing 10,000-repetition Gaussian distributions for each single case within the interval of uncertainty of a given stage, defined by the pre-determined means and standard deviations of each case, and calculating the mean and the standard deviations of the 10,000 randomly generated sets. This procedure was also implemented to include the associated errors to each $\delta^{13}C_{leaf}$, $\delta^{13}C_{CO2}$ and $\Delta^{13}C_{leaf}$ values into the aforementioned equations to account for all sources of error in the resolution of pCO_2 estimates.

References

1. Royer, D. L., Berner, R. A., Montañez, I. P., Tabor, N. J. & Beerling, D. J. CO_2 as a primary driver of phanerozoic climate. *GSA Today* **14**, 4–10 (2004).
2. Breecker, D. O., Sharp, Z. D. & McFadden, L. D. Atmospheric CO_2 concentrations during ancient greenhouse climates were similar to those predicted for AD 2100. *Proc. Natl. Acad. Sci.* **107**, 576–580 (2010).
3. Royer, D. L., Donnadieu, Y., Park, J., Kowalczyk, J. & Goddéris, Y. Error analysis of CO_2 and O_2 estimates from the long-term geochemical model GEOCARBSULF. *Am. J. Sci.* **314**, 1259–1283 (2014).
4. Poulsen, C. J., Tabor, C. & White, J. D. Long-term climate forcing by atmospheric oxygen concentrations. *Science* **348**, 1238–1241 (2015).
5. Peppe, D. J. & Royer, D. L. Can climate feel the pressure? *Science* **348**, 1210–1211 (2015).

6. Kidder, D. L. & Worsley, T. R. Phanerozoic large igneous provinces (LIPs), HEATT (haline euxinic acidic thermal transgression) episodes, and mass extinctions. *Palaeogeogr. Palaeoclimatol. Palaeoecol.* **295**, 162–191 (2010).
7. Barclay, R. S., McElwain, J. C. & Sageman, B. B. Carbon sequestration activated by a volcanic CO_2 pulse during Ocean Anoxic Event 2. *Nat. Geosci.* **3**, 205–208 (2010).
8. Huang, C. M., Retallack, G. J. & Wang, C. S. Early Cretaceous atmospheric pCO_2 levels recorded from pedogenic carbonates in China. *Cretac. Res.* **33**, 42–49 (2012).
9. Huang, C., Retallack, G. J., Wang, C. & Huang, Q. Paleoatmospheric pCO_2 fluctuations across the Cretaceous–Tertiary boundary recorded from paleosol carbonates in NE China. *Palaeogeogr. Palaeoclimatol. Palaeoecol.* **385**, 95–105 (2013).
10. Li, J., Wen, X. Y. & Huang, C. M. Lower Cretaceous paleosols and paleoclimate in Sichuan Basin, China. *Cretac. Res.* **62**, 154–171 (2016).
11. Martin, J. E., Amiot, R., Lécuyer, C. & Benton, M. J. Sea surface temperature contributes to marine crocodylomorph evolution. *Nat. Commun.* **5** (2014).
12. Mutterlose, J., Bottini, C., Schouten, S. & Damsté, J. S. S. High sea-surface temperatures during the early Aptian Oceanic Anoxic Event 1a in the Boreal Realm. *Geology* **42**, 439–442 (2014).
13. Naafs, B. D. A. & Pancost, R. D. Sea-surface temperature evolution across Aptian Oceanic Anoxic Event 1a. *Geology* **44**, 959–962 (2016).
14. Erba, E. Calcareous nannofossils and Mesozoic oceanic anoxic events. *Mar. Micropaleontol.* **52**, 85–106 (2004).
15. Jarvis, I. A. N., Gale, A. S., Jenkyns, H. C. & Pearce, M. A. Secular variation in Late Cretaceous carbon isotopes: a new $\delta^{13}C$ carbonate reference curve for the Cenomanian–Campanian (99.6–70.6 Ma). *Geol. Mag.* **143**, 561–608 (2006).
16. Barral, A., Gomez, B., Legendre, S. & Lécuyer, C. Evolution of the carbon isotope composition of atmospheric CO_2 throughout the Cretaceous. *Palaeogeogr. Palaeoclimatol. Palaeoecol.* **471**, 40–47 (2017).
17. Cerling, T. E. In *Palaeoweathering, palaeosurfaces and related continental deposits* (eds. Thiry, M. & Simon-Coinçon, R.) International Association of Sedimentologists Special Publication **27**, 43–60 (1999).
18. Jenkyns, H. C. Geochemistry of oceanic anoxic events. *Geochem. Geophys. Geosystems* **11** (2010).
19. Schubert, B. A. & Jahren, A. H. The effect of atmospheric CO_2 concentration on carbon isotope fractionation in C_3 land plants. *Geochim. Cosmochim. Acta* **96**, 29–43 (2012).
20. Franks, P. J. *et al*. New constraints on atmospheric CO_2 concentration for the Phanerozoic. *Geophys. Res. Lett.* **41**, 4685–4694 (2014).
21. Schubert, B. A. & Jahren, A. H. Global increase in plant carbon isotope fractionation following the Last Glacial Maximum caused by increase in atmospheric pCO_2. *Geology* **43**, 435–438 (2015).
22. Bocherens, H., Friis, E., Mariotti, A. & Pedersen, K. R. Carbon isotopic abundances in Mesozoic and Cenozoic fossil plants: Palaeoecological implications. *Lethaia* **26**, 347–358 (1993).
23. De Leeuw, J. W., Frewin, N. L., Van Bergen, P. F., Damsté, J. S. & Collinson, M. E. In *Mar*ine palae*o*envir*onmental analysis from fossils* (eds. Bosence, D. W. J. & Allison, P. A.) 83, 43–71 (Geological Society Special Publications, 1995).
24. Arens, N. C., Jahren, A. H. & Amundson, R. Can C_3 plants faithfully record the carbon isotopic composition of atmospheric carbon dioxide? *Paleobiology* **26**, 137–164 (2000).
25. Barral, A., Lécuyer, C., Gomez, B., Fourel, F. & Daviero-Gomez, V. Effects of chemical preparation protocols on $\delta^{13}C$ values of plant fossil samples. *Palaeogeogr. Palaeoclimatol. Palaeoecol.* **438**, 267–276 (2015).
26. Crafts-Brandner, S. J. & Salvucci, M. E. Rubisco activase constrains the photosynthetic potential of leaves at high temperature and CO_2. *Proc. Natl. Acad. Sci.* **97**, 13430–13435 (2000).
27. Falkowski, P. *et al*. The global carbon cycle: a test of our knowledge of Earth as a system. *Science* **290**, 291–296 (2000).
28. McElwain, J. C., Montañez, I., White, J. D., Wilson, J. P. & Yiotis, C. Was atmospheric CO_2 capped at 1000ppm over the past 300 million years? *Palaeogeogr. Palaeoclimatol. Palaeoecol.* **441**, 653–658 (2016).
29. Franks, P. J. & Royer, D. L. Comment on 'Was atmospheric CO_2 capped at 1000ppm over the past 300 million years?' by McElwain J. C. *et al*. [Palaeogeography, Palaeoclimatology, Palaeoecology 441 (2016) 653–658]. *Palaeogeogr. Palaeoclimatol. Palaeoecol*. (2017).
30. McElwain, J. C., Montañez, I. P., White, J. D., Wilson, J. P. & Yiotis, C. Reply to Comment on 'Was atmospheric CO_2 capped at 1000ppm over the past 300 million years?'[Palaeogeography, Palaeoclimatology, Palaeoecology 441 (2016) 653–658]. *Palaeogeogr. Palaeoclimatol. Palaeoecol*. (2017).
31. Wang *et al*. Paleo-CO_2 variation trends and the Cretaceous greenhouse climate. *Earth-Sci. Rev.* **129**, 136–147 (2014).
32. Pearson, P. N. & Palmer, M. R. Middle Eocene seawater pH and atmospheric carbon dioxide concentrations. *Science* **284**, 1824–1826 (1999).
33. Pearson, P. N. & Palmer, M. R. Atmospheric carbon dioxide concentrations over the past 60 million years. *Nature* **406**, 695–699 (2000).
34. Lécuyer, C., Grandjean, P., Reynard, B., Albarède, F. & Telouk, P. $^{11}B/^{10}B$ analysis of geological materials by ICP–MS Plasma 54: Application to the boron fractionation between brachiopod calcite and seawater. *Chem. Geol.* **186**, 45–55 (2002).
35. Simon, L., Lécuyer, C., Maréchal, C. & Coltice, N. Modelling the geochemical cycle of boron: implications for the long-term $\delta^{11}B$ evolution of seawater and oceanic crust. *Chem. Geol.* **225**, 61–76 (2006).
36. Kiessling, W. & Simpson, C. On the potential for ocean acidification to be a general cause of ancient reef crises. *Glob. Change Biol.* **17**, 56–67 (2011).
37. Erba, E., Bottini, C., Weissert, H. J. & Keller, C. E. Calcareous nannoplankton response to surface-water acidification around Oceanic Anoxic Event 1a. *Science* **329**, 428–432 (2010).
38. Arkhipkin, A. I. & Laptikhovsky, V. V. Impact of ocean acidification on plankton larvae as a cause of mass extinctions in ammonites and belemnites. *Neues Jahrb. Geol. Paläontol.-Abh.* **266**, 39–50 (2012).
39. Wagner, T., Wallmann, K., Herrle, J. O., Hofmann, P. & Stuesser, I. Consequences of moderate 25,000 yr lasting emission of light CO_2 into the mid-Cretaceous ocean. *Earth Planet. Sci. Lett.* **259**, 200–211 (2007).
40. Schlanger, S. O. & Jenkyns, H. C. Cretaceous oceanic anoxic events: causes and consequences. *Neth. J. Geosci. En Mijnb.* **55**, 179–184 (1976).
41. Kuypers, M. M., Pancost, R. D., Nijenhuis, I. A. & Sinninghe Damsté, J. S. Enhanced productivity led to increased organic carbon burial in the euxinic North Atlantic basin during the late Cenomanian oceanic anoxic event. *Paleoceanography* **17**, 1051 (2002).
42. Adams, D. D., Hurtgen, M. T. & Sageman, B. B. Volcanic triggering of a biogeochemical cascade during Oceanic Anoxic Event 2. *Nat. Geosci.* **3**, 201–204 (2010).
43. Gomes, M. L., Hurtgen, M. T. & Sageman, B. B. Biogeochemical sulfur cycling during Cretaceous oceanic anoxic events: a comparison of OAE1a and OAE2. *Paleoceanography* (2016).
44. Tessin, A., Sheldon, N. D., Hendy, I. & Chappaz, A. Iron limitation in the Western Interior Seaway during the Late Cretaceous OAE 3 and its role in phosphorus recycling and enhanced organic matter preservation. *Earth Planet. Sci. Lett.* **449**, 135–144 (2016).
45. Leckie, R. M., Bralower, T. J. & Cashman, R. Oceanic anoxic events and plankton evolution: Biotic response to tectonic forcing during the mid-Cretaceous. *Paleoceanography* **17**, 13–1 (2002).
46. Hay, W. W. Evolving ideas about the Cretaceous climate and ocean circulation. *Cretac. Res.* **29**, 725–753 (2008).
47. Hasegawa *et al*. Drastic shrinking of the Hadley circulation during the mid-Cretaceous Supergreenhouse. *Clim. Past* **8**, 1323–1337 (2012).
48. Adams, J. M., Faure, H., Faure-Denard, L., McGlade, J. M. & Woodward, F. I. Increases in terrestrial carbon storage from the Last Glacial Maximum to the present. *Nature* **348**, 711714 (1990).

49. Montañez *et al*. Climate, pCO_2 and terrestrial carbon cycle linkages during late Palaeozoic glacial–interglacial cycles. *Nat. Geosci.* **9**, 824–828 (2016).
50. National Oceanic and Atmospheric Administration, Earth System Research Laboratory, Global Monitoring Division. U.S. Department of Commerce. http://www.esrl.noaa.gov/.
51. Chaboureau, A.-C., Sepulchre, P., Donnadieu, Y. & Franc, A. Tectonic-driven climate change and the diversification of angiosperms. *Proc. Natl. Acad. Sci.* **111**, 14066–14070 (2014).
52. Gomez, B., Martín-Closas, C., Barale, G., Thévenard, F. & Guignard, G. *Frenelopsis* (Coniferales: Cheirolepidiaceae) and related male organ genera from the Lower Cretaceous of Spain. *Palaeontology* **45**, 997–1036 (2002).
53. Gomez, B. *et al*. Floristic assemblage from the Albian-Cenomanian of Charente-Maritime (SW France). *Ann. Paléontol.* **90**, 147–159 (2004).
54. Mendes, M. M., Dinis, J. L., Gomez, B. & Pais, J. Reassessment of the cheirolepidiaceous conifer *Frenelopsis teixeirae* Alvin et Pais from the Early Cretaceous (Hauterivian) of Portugal and palaeoenvironmental considerations. *Rev. Palaeobot. Palynol.* **161**, 30–42 (2010).
55. Barral, A. *et al*. Local-scale analysis of plant community from the Early Cretaceous riparian ecosystem of Hautrage, Belgium. *Palaeogeogr. Palaeoclimatol. Palaeoecol.* **443**, 107–122 (2016).
56. Nguyen, T. T. T. *et al*. Ecological distribution of Cenomanian terrestrial plants based on $^{13}C/^{12}C$ ratios. *Palaeogeogr. Palaeoclimatol. Palaeoecol.* **145**, 79–93 (1999).
57. Nguyen, T. T. T. *et al*. Isotope reconstruction of plant palaeoecology. Case study of Cenomanian floras from Bohemia. *Palaeogeogr. Palaeoclimatol. Palaeoecol.* **183**, 43–70 (2002).
58. Farquhar, G. D., Ehleringer, J. R. & Hubick, K. T. Carbon isotope discrimination and photosynthesis. *Annu. Rev. Plant Biol.* **40**, 503–537 (1989).

Acknowledgements

This work was financially supported by the CNRS-UMR 5276 and the projects CGL2013-42643-P, CGL2014-52163-C2, CGL2015-68363-P and CGL2015-60805-P funded by the Ministerio de Economía y Competitividad of the Spanish government and 2014SGR-251 funded by the AGAUR, Catalan Research Authority.

Author Contributions

A.B. conceived the original idea for this study and led the writing of the manuscript under the advising of B.G. and C.L. Plant fossil materials were provided by B.G. and V.D.-G. $\delta^{13}C_{leaf}$ measurements were made by A.B., F.F. and C.L. All the authors contributed to data interpretation and manuscript editing.

Additional Information

Supplementary information accompanies this paper at doi:10.1038/s41598-017-08234-0

Competing Interests: The authors declare that they have no competing interests.

Publisher's note: Springer Nature remains neutral with regard to jurisdictional claims in published maps and institutional affiliations.